

Precision nephrology identified tumor necrosis factor activation variability in minimal change disease and focal segmental glomerulosclerosis

OPEN

Laura H. Mariani^{1,45}, Sean Eddy^{1,45}, Fadhl M. AlAkwa¹, Phillip J. McCown¹, Jennifer L. Harder¹, Viji Nair¹, Felix Eichinger¹, Sebastian Martini¹, Adebowale D. Ademola², Vincent Boima³, Heather N. Reich⁴, Jamal El Saghir¹, Bradley Godfrey¹, Wenjun Ju¹, Emily C. Tanner¹, Virginia Vega-Warner¹, Noel L. Wys¹, Sharon G. Adler⁵, Gerald B. Appel⁶, Ambarish Athavale⁷, Meredith A. Atkinson⁸, Serena M. Bagnasco⁹, Laura Barisoni¹⁰, Elizabeth Brown¹¹, Daniel C. Cattran⁴, Gaia M. Coppock¹², Katherine M. Dell¹³, Vimal K. Derebail¹⁴, Fernando C. Fervenza¹⁵, Alessia Fornoni¹⁶, Crystal A. Gadegbeku¹⁷, Keisha L. Gibson¹⁸, Laurence A. Greenbaum¹⁹, Sangeeta R. Hingorani²⁰, Michelle A. Hladunewich⁴, Jeffrey B. Hodgin²¹, Marie C. Hogan¹⁵, Lawrence B. Holzman¹², J. Ashley Jefferson²², Frederick J. Kaskel²³, Jeffrey B. Kopp²⁴, Richard A. Lafayette²⁵, Kevin V. Lemley²⁶, John C. Lieske¹⁵, Jen-Jar Lin²⁷, Rajarasee Menon²⁸, Kevin E. Meyers²⁹, Patrick H. Nachman³⁰, Cynthia C. Nast³¹, Michelle M. O'Shaughnessy³², Edgar A. Otto¹, Kimberly J. Reidy²³, Kamalanathan K. Sambandam^{11,33}, John R. Sedor^{34,35,36,37}, Christine B. Sethna³⁸, Pamela Singer³⁸, Tarak Srivastava³⁹, Cheryl L. Tran⁴⁰, Katherine R. Tuttle^{22,41}, Suzanne M. Vento⁴², Chia-shi Wang¹⁹, Akinlolu O. Ojo⁴³, Dwomoa Adu³, Debbie S. Gipson⁴⁴, Howard Trachtman¹ and Matthias Kretzler^{1,28}

¹Division of Nephrology, Department of Internal Medicine, University of Michigan, Ann Arbor, Michigan, USA; ²Department of Paediatrics, Faculty of Clinical Sciences, College of Medicine, University of Ibadan, Ibadan, Oyo State, Nigeria; ³Department of Medicine and Therapeutics, University of Ghana Medical School, College of Health Sciences, University of Ghana, Accra, Ghana; ⁴Division of Nephrology, Department of Medicine, University Health Network and University of Toronto, Toronto, Ontario, Canada; ⁵Division of Nephrology and Hypertension at Harbor-UCLA Medical Center and The Lundquist Institute for Biomedical Innovation, Torrance, California, USA; ⁶Division of Nephrology, Department of Medicine, Columbia University Irving Medical Center, New York, New York, USA; ⁷Division of Nephrology-Hypertension, University of San Diego, California, San Diego, California, USA; ⁸Division of Pediatric Nephrology, Johns Hopkins University School of Medicine, Baltimore, Maryland, USA; ⁹Department of Pathology, Johns Hopkins University School of Medicine, Baltimore, Maryland, USA; ¹⁰Department of Pathology and Medicine, Division of Nephrology, Duke University School of Medicine, Durham, North Carolina, USA; ¹¹Division of Nephrology, Department of Pediatrics, University of Texas Southwestern Medical Center, Dallas, Texas, USA; ¹²Renal-Electrolyte and Hypertension Division, Perelman School of Medicine, University of Pennsylvania, Philadelphia, Pennsylvania, USA; ¹³Center for Pediatric Nephrology, Cleveland Clinic, Case Western Reserve University, Cleveland, Ohio, USA; ¹⁴University of North Carolina Kidney Center, Division of Nephrology and Hypertension, University of North Carolina at Chapel Hill, Chapel Hill, North Carolina, USA; ¹⁵Division of Nephrology and Hypertension, Department of Internal Medicine, Mayo Clinic, Rochester, Minnesota, USA; ¹⁶Katz Family Division of Nephrology and Hypertension, Department of Medicine, University of Miami Miller School of Medicine, Miami, Florida, USA; ¹⁷Department of Kidney Medicine, Glickman Urological and Kidney Institute, Cleveland Clinic, Cleveland, Ohio, USA; ¹⁸Pediatric Nephrology Division, School of Medicine, University of North Carolina, Chapel Hill, North Carolina, USA; ¹⁹Division of Nephrology, Department of Pediatrics, Emory University School of Medicine, Atlanta, Georgia, USA; ²⁰Division of Nephrology, Department of Pediatrics, University of Washington, Seattle, Washington, USA; ²¹Department of Pathology, University of Michigan, Ann Arbor, Michigan, USA; ²²Division of Nephrology, Department of Medicine, University of Washington, Seattle, Washington, USA; ²³Division of Pediatric Nephrology, Montefiore Medical Center, Bronx, New York, USA; ²⁴National Institute of Diabetes and Digestive Diseases, National Institutes of Health, Bethesda, Maryland, USA; ²⁵Department of Medicine, Division of Nephrology, Stanford University, Stanford, CA, USA; ²⁶Department of Pediatrics, Keck School of Medicine of the University of Southern California, Los Angeles, California, USA; ²⁷Department of Pediatrics, Wake Forest University School of Medicine, Winston-Salem, North Carolina, USA; ²⁸Department of Computational Medicine and Bioinformatics, University of Michigan, Ann Arbor, Michigan, USA; ²⁹Division of Nephrology, Children's Hospital of Philadelphia, Philadelphia, Pennsylvania, USA; ³⁰Division of Nephrology and Hypertension, Department of Medicine, University of Minnesota, Minneapolis, Minnesota, USA; ³¹Department of Pathology, Cedars-Sinai Medical Center, Los Angeles, California, USA; ³²Department of Medicine, Division of Renal Medicine, Cork University Hospital, Cork, Ireland; ³³Division of Nephrology, Department of Internal Medicine, University of Texas Southwestern Medical Center, Dallas, Texas, USA; ³⁴Lerner Research Institutes, Cleveland Clinic,

Correspondence: Matthias Kretzler, University of Michigan, MSRB II, 4544-D, 1150 West Medical Center Drive, Ann Arbor, Michigan 48109, USA. E-mail: kretzler@umich.edu; or Laura H. Mariani, Department of Internal Medicine, Division of Nephrology, University of Michigan, MSRB II, 4544-C, 1150 West Medical Center Drive, Ann Arbor, Michigan 48109, USA. E-mail: lmariani@med.umich.edu

⁴⁵LHM and SE are co-first authors.

Received 8 February 2022; revised 25 October 2022; accepted 28 October 2022

Cleveland, Ohio, USA; ³⁵Department of Molecular Medicine, Case Western Reserve University, Cleveland, Ohio, USA; ³⁶Department of Physiology, Case Western Reserve University, Cleveland, Ohio, USA; ³⁷Department of Biophysics, Case Western Reserve University, Cleveland, Ohio, USA; ³⁸Division of Pediatric Nephrology, Cohen Children's Medical Center, New Hyde Park, New York, USA; ³⁹Section of Nephrology, Children's Mercy Hospital, Kansas City, Missouri, USA; ⁴⁰Pediatric Nephrology, Mayo Clinic, Rochester, Minnesota, USA; ⁴¹Providence Medical Research Center, Providence Health Care, University of Washington, Spokane, Washington, USA; ⁴²Division of Nephrology, Department of Pediatrics, New York University School of Medicine, New York, New York, USA; ⁴³Department of Population Health, School of Medicine, University of Kansas Medical Center, Kansas City, Kansas, USA; and ⁴⁴Division of Nephrology, Department of Pediatrics, University of Michigan, Ann Arbor, Michigan, USA

The diagnosis of nephrotic syndrome relies on clinical presentation and descriptive patterns of injury on kidney biopsies, but not specific to underlying pathobiology. Consequently, there are variable rates of progression and response to therapy within diagnoses. Here, an unbiased transcriptomic-driven approach was used to identify molecular pathways which are shared by subgroups of patients with either minimal change disease (MCD) or focal segmental glomerulosclerosis (FSGS). Kidney tissue transcriptomic profile-based clustering identified three patient subgroups with shared molecular signatures across independent, North American, European, and African cohorts. One subgroup had significantly greater disease progression (Hazard Ratio 5.2) which persisted after adjusting for diagnosis and clinical measures (Hazard Ratio 3.8). Inclusion in this subgroup was retained even when clustering was limited to those with less than 25% interstitial fibrosis. The molecular profile of this subgroup was largely consistent with tumor necrosis factor (TNF) pathway activation. Two TNF pathway urine markers were identified, tissue inhibitor of metalloproteinases-1 (TIMP-1) and monocyte chemoattractant protein-1 (MCP-1), that could be used to predict an individual's TNF pathway activation score. Kidney organoids and single-nucleus RNA-sequencing of participant kidney biopsies, validated TNF-dependent increases in pathway activation score, transcript and protein levels of TIMP-1 and MCP-1, in resident kidney cells. Thus, molecular profiling identified a subgroup of patients with either MCD or FSGS who shared kidney TNF pathway activation and poor outcomes. A clinical trial testing targeted therapies in patients selected using urinary markers of TNF pathway activation is ongoing.

Kidney International (2022) ■, ■-■; <https://doi.org/10.1016/j.kint.2022.10.023>

KEYWORDS: data integration; nephrotic syndrome; TNF; transcriptomics
Copyright © 2022, International Society of Nephrology. Published by Elsevier Inc. This is an open access article under the CC BY-NC-ND license (<http://creativecommons.org/licenses/by-nc-nd/4.0/>).

Nephrotic syndrome is characterized by proteinuria, hypoalbuminemia, hyperlipidemia, and edema. Two nephrotic diseases, minimal change disease (MCD) and focal segmental glomerulosclerosis (FSGS), currently diagnosed based on histopathologic features, have broadly overlapping clinical presentations and treatment approaches.¹

Within each diagnosis, however, some patients respond well to current therapy, whereas others either do not respond or relapse upon stopping therapy with variable risk of loss of kidney function. These clinical observations suggest a heterogeneous biology underlying current disease classification.²⁻⁴ Because of limited understanding of pathobiology, interpretation of the clinical outcome variability in observational studies and clinical trials is challenging,^{5,6} and molecularly-driven,^{7,8} personalized⁶ treatments for MCD and FSGS are unavailable.

Nevertheless, nephrotic syndrome is well positioned for implementing precision medicine. Clinically procured kidney biopsy tissue allows for unbiased identification of molecular signatures that can be linked to histopathology, noninvasive biomarkers, and evaluated against clinical outcomes. With the goal of identifying molecular pathways that are shared by subgroups of patients with MCD and FSGS, this study implemented a multidimensional data integration approach (Figure 1) in the prospective North American Nephrotic Syndrome Study Network (NEPTUNE),⁹ then replicated in the European Renal cDNA Bank (ERCB)^{10,11} and the Human Heredity and Health in Africa Kidney Disease Research Network cohort (H3Africa).^{12,13}

The study aims to agnostically identify groups of patients with shared molecular signatures, to identify the relevant pathways from that signature that could then be evaluated in individual patients using potential noninvasive markers. Such markers of the disease mechanism may enable targeted therapeutic interventions.

METHODS

Study participants

The study included 220 NEPTUNE,⁹ 35 H3Africa,¹² and 30 ERCB^{10,11} participants with biopsy-proven MCD or FSGS and compartment-enriched genome-wide kidney mRNA expression profiles.

NEPTUNE (NCT01209000) is a prospective study of children and adults with proteinuria, recruited from 21 sites at the time of their first clinically indicated kidney biopsy.^{9,14} ERCB is a European study of adults recruited at 28 sites, with biopsy tissue for gene expression profiling and cross-sectional clinical information, at the time of a clinically indicated kidney biopsy.^{10,11} H3Africa¹² is a prospective study of participants aged 15 years and above, eligible for a kidney biopsy, recruited from 13 clinical centers in Nigeria and Ghana with an estimated glomerular filtration rate (eGFR) of ≥ 15 ml/min per 1.73 m² and proteinuria (albuminuria >500 mg/d).¹²

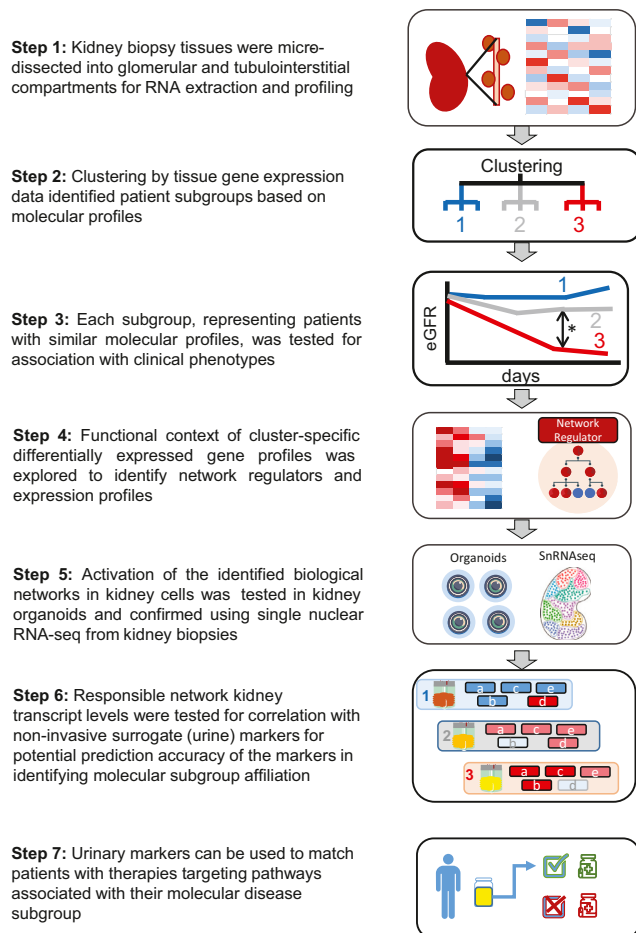


Figure 1 | Analysis strategy. Flowchart of tubulointerstitial compartment gene expression to identify molecular subgroups and associated noninvasive urinary markers. eGFR, estimated glomerular filtration rate; snRNA-seq, single-nucleus RNA sequencing.

For all cohorts, informed consent was obtained from individual patients or parents/guardians on approval by institutional review boards or local ethics committees of participating institutions.

Clinical data

NEPTUNE participants were followed 2 to 3 times per year, for up to 5 years. Medical history, medication use, laboratory results, blood and urine samples for the measurement of serum creatinine, and urine protein-to-creatinine ratio (UPCR) were collected at each study visit. eGFR (ml/min per 1.73 m²) was calculated using the Chronic Kidney Disease Epidemiology Collaboration formula for participants ≥ 18 years old and the modified chronic kidney disease in children-Schwartz formula for participants < 18 years old, with an average taken for young adults aged 18 to 26 years.^{15–17} The endpoint of kidney functional loss was defined by a 40% reduction in eGFR or the onset of kidney failure (initiation of dialysis, receipt of kidney transplant or eGFR < 15 ml/min per 1.73 m² measured at 2 sequential visits).¹⁸ Complete remission was defined as UPCR < 0.3 mg/mg on a single-void urine or a 24-hour urine collection. In ERCB and H3Africa, clinical information, including demographics and clinical laboratory results, was obtained at the time of biopsy.

Kidney pathology

Diagnosis in NEPTUNE was assigned by study pathologists based on biopsy reports and/or digital images. The degree of interstitial fibrosis (IF) was visually assessed and scored by 2 to 5 pathologists using biopsy whole slide images of trichrome, periodic acid–Schiff, or silver-stained sections, recorded as the percent of cortex involved, and averaged across the pathologists' measures.^{19,20}

Transcriptome profiling

In NEPTUNE, RNA sequencing (RNA-seq) was performed on manually microdissected kidney biopsy tissue that separated tubulointerstitial and glomerular compartments of the research core. For H3Africa, a 5-mm cortical segment (not needed for clinical diagnosis) was manually microdissected, RNA-isolated, and sequenced to generate RNA-seq profiles (see [Supplementary Methods](#)).

In ERCB, compartment-specific transcriptomic profiles of the research core were generated using the Affymetrix microarray platform. NEPTUNE RNA-seq and ERCB microarray data are available at [Nephroseq.org](#) and through Gene Expression Omnibus²¹ (GSE219195, GSE197307, GSE104954, GSE104948).

Cluster analysis, differential expression, and functional enrichment analysis

R Software (R Core Team [2013]) was used for Kmeans, Prediction Analysis of Microarrays (PAM), and hierarchical clustering analyses.^{22,23} Optimal clustering was determined using delta-K and the ConsensusClusterPlus package.²² The linear models for microarray data (limma) package²⁴ was used for differential expression analysis. Differentially expressed genes (absolute fold change > 1.5 and q value < 0.05) between clusters were analyzed for the enrichment of canonical pathways using the Ingenuity Pathway Analysis Software Suite (IPA; Qiagen).²⁵ Previously published²⁶ single-cell RNA-seq cell-type selective expression clusters from adult reference kidney tissue can be accessed at <http://nephrocell.miktmc.org/> and GEO (GSE14098).

Tumor necrosis factor activation score

A tumor necrosis factor (TNF) activation network was generated from expert curated interactions from NETPro annotations in the Genomatix Genome Analyzer database (Precigen Bioinformatics). From the database, 272 causally downstream genes or proteins that increased expression from TNF exposure were used to generate a TNF activation score. Individual gene expression values were first Z-transformed. The TNF activation score for each participant was the average Z-score of the 272 genes in their kidney RNA-seq profile.

Urine marker profiling

Urine proteins were identified and measured using the multiplex Luminex platform (Eve Technologies) composed of a panel of 54 urinary cytokines, matrix metalloproteinases, and tissue inhibitor of metalloproteinases (see [Supplementary Methods](#)). A candidate protein had to satisfy the following criteria to be considered a potential noninvasive marker of TNF activation: (i) protein must be a product of a gene expressed downstream of TNF; (ii) urine protein expression must correlate with the corresponding kidney tissue gene expression (mRNA levels), and (iii) gene expression must correlate with the TNF activation score.

Putative urine markers were assayed in duplicate using Quantikine enzyme-linked immunosorbent assay kit human chemokine (C-C motif) ligand 2 (CCL2)/monocyte chemoattractant protein-1

(MCP-1) (DCP00) and tissue inhibitor of metalloproteinases 1 (TIMP-1) (DTM100; R&D Systems). Absorbance was measured with a VersaMax enzyme-linked immunosorbent assay plate reader, and results were calculated with SoftMax Pro (Molecular Devices). Markers were normalized to urine creatinine concentration and \log_2 transformed.

Statistical analysis of the association with clinical data and urine markers

Descriptive statistics were used to characterize baseline (time of biopsy) participant characteristics by molecular cluster. Differences in Kaplan-Meier curves, by molecular cluster, were tested by the log-rank test. Univariate Cox proportional hazards models were fit separately for time from biopsy to complete remission and time to the composite of end-stage kidney disease and a 40% decline in eGFR to assess the association of molecular cluster and TNF score with clinical outcomes. Models were adjusted for diagnosis (MCD, FSGS), eGFR, and UPCr. IF and glomerular sclerosis were assumed to be on the causal pathway and therefore not included in the models. Pearson's correlation was used to assess the relationship between the TNF score, marker tissue mRNA expression, and urinary concentration. Linear regression models were fit to assess the association of urinary markers and clinical features with TNF score, and to calculate a predicted score. Pearson's correlation was used to correlate the predicted and observed TNF activation scores. Analyses were performed using STATA, v12.1.

Single-nuclear RNA-seq

Nuclei were prepared from the biopsy tissue of 10 NEPTUNE participants (5 from cluster 3, with high TNF activity scores [defined as TNF High], and 5 from clusters 1 and 2, with lower TNF activity scores [defined as TNF Low]) stored in RNAlater using protocols from the Kidney Precision Medicine Project^{27,28} (Supplementary Methods, GSE213030). Nuclear cluster annotation was determined by defining enriched genes in each cell cluster and comparing cluster selective gene profiles with previously identified human kidney cell marker gene sets.^{26–28}

Kidney organoid culture, treatment, and analysis

Kidney organoids were generated from UM77-2 human embryonic stem cells as previously described.²⁹ Organoids were treated with TNF (R&D Systems, Cat# 10291-TA) resuspended in phosphate-buffered saline on day 23 at the indicated concentrations. Organoid supernatants were removed at specified times, RNA extracted, and sequenced (Supplementary Methods). Organoid culture supernatants and cell lysates were diluted 150-fold to measure MCP-1 and 10-fold to measure TIMP-1 using the enzyme-linked immunosorbent assay as described above. Quantitative real-time polymerase chain reaction analysis was performed in triplicate using TaqMan Fast Universal PCR Master Mix (2X) for CCL2, TIMP-1, and glyceraldehyde-3-phosphate dehydrogenase.

RESULTS

Unbiased consensus clustering of gene expression profiles identifies shared molecular signatures

Transcriptomic profiles of microdissected kidney biopsy compartments were used to group participants into distinct sub-clusters. Because of the known association of tubulointerstitial

changes with risk of loss of eGFR, tubulointerstitial transcriptional data were analyzed first. Transcriptomes from NEPTUNE participants clustered into 3 groups ($n = 85, 76,$ and $59,$ respectively), with 1 cluster (T3) demonstrating the highest cluster stability (Figure 2a). The delta-K revealed that the 3-cluster solution was optimal across clustering approaches (Supplementary Figure S1A–C). To validate the molecular profiles identified in NEPTUNE, Kmeans, PAM, and hierarchical consensus clustering^{22,23} were also applied to the tubulointerstitial transcriptome data from 2 independent FSGS/MCD cohorts, ERCB ($N = 30$) and H3Africa ($N = 35$), resulting in 3 distinct clusters (Figure 2b and c) with high cluster stability. Glomerular compartment clustering also identified 3 clusters (Supplementary Figure S2A and B), with a transcriptional signature largely shared with the tubulointerstitium (Figure 2d). Differential expression analysis of the tubulointerstitial transcripts between T3 and the other 2 clusters in each cohort showed a robust, directionally conserved molecular signal across cohorts (correlation of fold change 0.94, $P < 0.001$, for NEPTUNE vs. ERCB and 0.93, $P < 0.001$, for NEPTUNE vs. H3; Figure 2e and f). Finally, of the 179 NEPTUNE participants with measured IF, clustering was repeated in only those participants with IF $< 25\%$ ($n = 148$). All 26 participants, originally in T3 from this group, again clustered together.

NEPTUNE participants in T3 were older and had a lower eGFR, greater IF, and higher UPCr at biopsy (Table 1; Supplementary Figure S3). In ERCB and H3Africa, participants in T3 also had a lower eGFR and were older. Although T3 had a greater proportion of FSGS in all 3 cohorts, it also included participants with MCD (Figure 2g, Supplementary Figure S1D and E). In an unadjusted survival model, NEPTUNE T3 participants were more likely to reach the composite of end-stage kidney disease or a 40% decline in eGFR (unadjusted hazard ratio [HR]: 5.23 [95% confidence interval: 1.9, 14.5], $P < 0.001$, for overall differences in curves; Figure 2h) and fewer complete proteinuria remission events were observed (unadjusted HR: 0.73 [95% confidence interval: 0.43, 1.26], $P = 0.068$, for overall difference in curves; Figure 2i) compared with T1.

Biological and molecular relevance of cluster 3

Differential mRNA expression profiles were used to elucidate the molecular functions associated with cluster T3. In NEPTUNE, there were 2721 transcripts in T3 with an absolute 1.5-fold change and $q < 0.05$ (2199 upregulated, 522 downregulated) compared with T1 and T2 (Supplementary Table S1A). This gene set was analyzed to identify enriched canonical pathways, predicted upstream regulators,³⁰ and gene interaction networks. These analyses converged on TNF pathway activation.

In signal transduction pathway over-representation (enrichment), the granulocyte adhesion and diapedesis signal transduction pathway had the highest enrichment score ($-\log(p) = 21.4$). Of the 180 genes in this pathway, 70 (38.9%) were found differentially regulated in T3, including TNF (2.4-fold upregulated in T3, $q < 0.001$, Figure 3a²⁶).

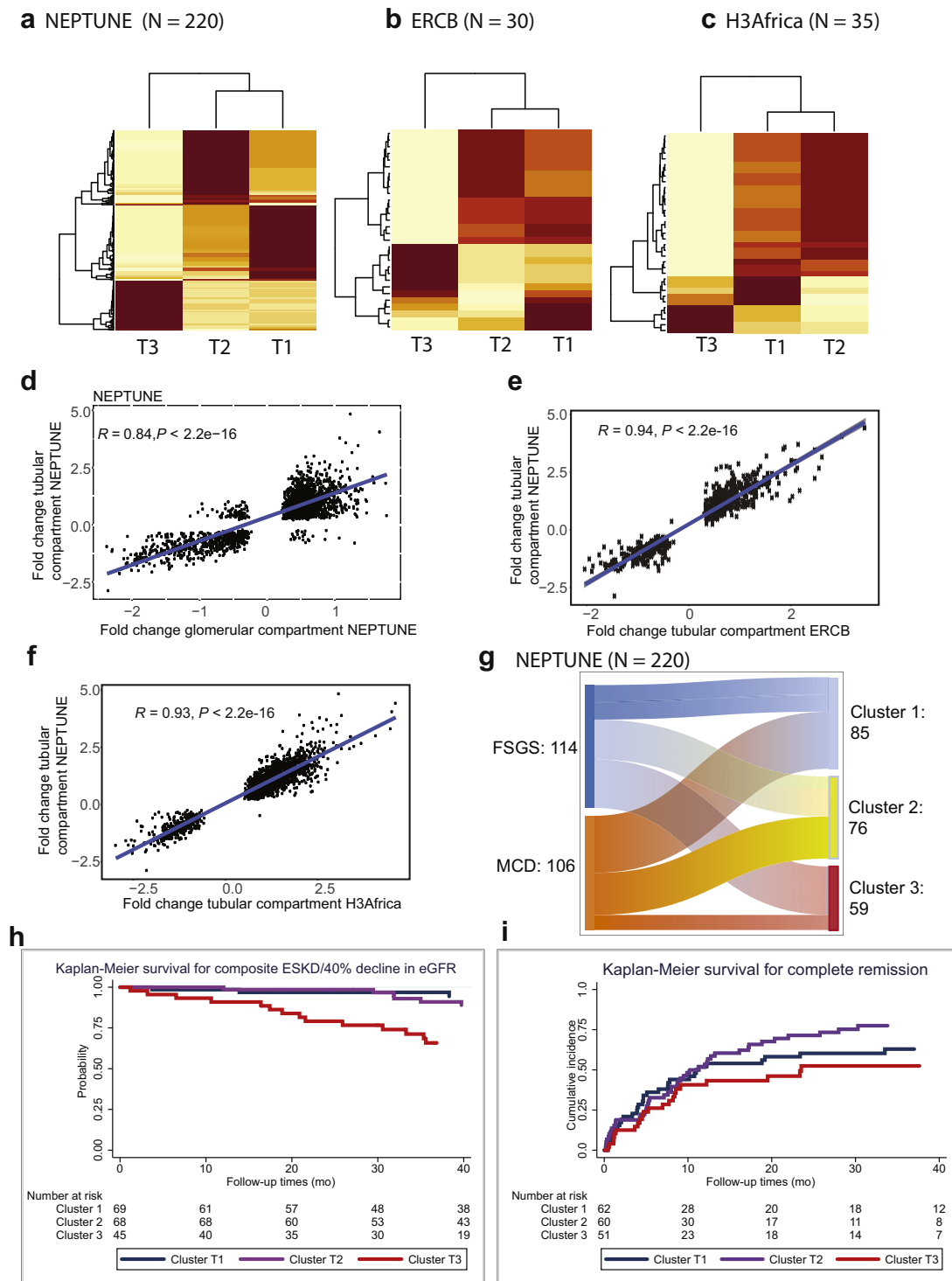


Figure 2 | Kidney transcriptomic cluster membership and unadjusted Kaplan-Meier curves. Consensus clustering using Kmeans identified optimal cluster membership from tubulointerstitial transcriptomic profiles with 3 clusters (clusters were designated by tissue compartment and cluster number, T1, T2, T3 for tubulointerstitial clusters) in a cluster matrix from (a) North American Nephrotic Syndrome Study Network (NEPTUNE), (b) European Renal cDNA Bank (ERCB), and (c) Human Heredity and Health in Africa Kidney Disease Research Network (H3Africa) cohorts. The values ranged from 0 (pale yellow, samples do not cluster together) to 1 (brown, samples demonstrate high affinity and cluster together). Scatter plots show a strong correlation of significant fold change differences of genes differentially expressed in (d) tubulointerstitial and glomerular compartments in NEPTUNE; (e) tubulointerstitial cluster 3 (T3) compared with T2 and T1 from NEPTUNE (y-axis) and cluster T3 compared with T1 and T2 from ERCB (x-axis); and, similarly, for (f) H3Africa (x-axis). (g) Alluvial plot of correspondence between the diagnosis and cluster membership of participants in the NEPTUNE cohort. Unadjusted Kaplan-Meier survival curves by the NEPTUNE tubulointerstitial cluster for (h) composite endpoint of 40% loss of estimated glomerular filtration rate (eGFR) or end-stage kidney disease (ESKD) and (i) complete remission. FSGS, focal segmental glomerulosclerosis; UPCR, urine protein-to-creatinine ratio.

Table 1 | Clinical characteristics of participants summarized by cluster identity and cohort

NEPTUNE	All (N = 220)	Cluster 1 (N = 85)	Cluster 2 (N = 76)	Cluster 3 (N = 59)	P value
Age, mean (SD)	28.2 (21.7)	22.3 (19.5)	26.8 (22.6)	38.5 (20.0)	<0.0001
Female, n (%)	89 (40)	33 (39)	30 (39)	26 (44)	0.82
Adult, n (%)	112 (59)	31 (36)	35 (46)	46 (78)	<0.0001
eGFR, mean (SD)	89.5 (46.8)	102.1 (40.7)	104.2 (48.9)	52.3 (29.2)	<0.0001
Albumin, mean (SD)	3.62 (0.89)	3.68 (0.86)	3.62 (0.89)	3.54 (0.95)	0.3916
FSGS, n (%)	114 (52)	32 (38)	37 (49)	45 (76)	<0.0001
UPCR, median (IQR)	2.76 (1.0, 7.04)	1.9 (0.6, 7.1)	2.56 (1.02, 5.5)	5.35 (2.0, 10.6)	<0.0001
% IF, median (IQR)	4 (0, 16)	1.5 (0, 5)	3 (0, 8)	20 (10, 55)	<0.0001
Disease duration before biopsy, mo, mean (SD)	29.47 (69.46)	26.78 (46.56)	18 (50.6)	49 (108)	0.30
On RAAS blockade, n (%)	86 (39)	34 (40)	26 (34)	26 (44)	0.0005
On IST, n (%)	101 (46)	49 (58)	37 (49)	15 (25)	0.0005
ERCB	Cluster 1 (N = 18)	Cluster 2 (N = 4)	Cluster 3 (N = 8)	P value	
Age, mean (SD)	42.2 (19.0)	29.4 (6.6)	49.2 (18.3)	0.63	
Female, n (%)	10 (56)	1 (25)	3 (38)	0.59	
eGFR, mean (SD)	92.2 (34.5)	119.0 (4.0)	43.2 (31.0)	0.02	
FSGS, n (%)	8 (44)	2 (50)	7 (87)	0.135	
H3Africa	Cluster 1 (N = 14)	Cluster 2 (N = 16)	Cluster 3 (N = 5)	P value	
Age, mean (SD)	24.1 (10.2)	30.0 (14.1)	30.8 (10.7)	0.19	
Female, n (%)	3 (21)	4 (25)	0 (0)	0.90	
eGFR, mean (SD)	89.8 (42.6)	109.8 (14.7)	25.8 (11.7)	0.03	
FSGS, n (%)	7 (50)	4 (25)	4 (80)	0.07	
UPCR, median (IQR)	1.4 (1.1, 2.2)	1.1 (0.3, 2.8)	3.6 (1.8, 7.5)	0.05	
% IF, median (IQR)	0 (0, 9)	0 (0, 1)	40 (0, 40)	0.01	
Disease duration less than 6 mo, n (%)	2 (14)	4 (25)	4 (80)	0.02	
IST in the past 6 mo, n (%)	5 (36)	4 (25)	1 (20)	0.71	

eGFR, estimated glomerular filtration rate (ml/min per 1.73 m²); ERCB, European Renal cDNA Bank; FSGS, focal segmental glomerulosclerosis; H3Africa, Human Heredity and Health in Africa Kidney Disease Research Network cohort; IF, interstitial fibrosis; IQR, interquartile range; IST, immunosuppressive therapy; NEPTUNE, North American Nephrotic Syndrome Study Network; RAAS, renin angiotensin aldosterone system; UPCR, urine protein-to-creatinine ratio (mg/mg).

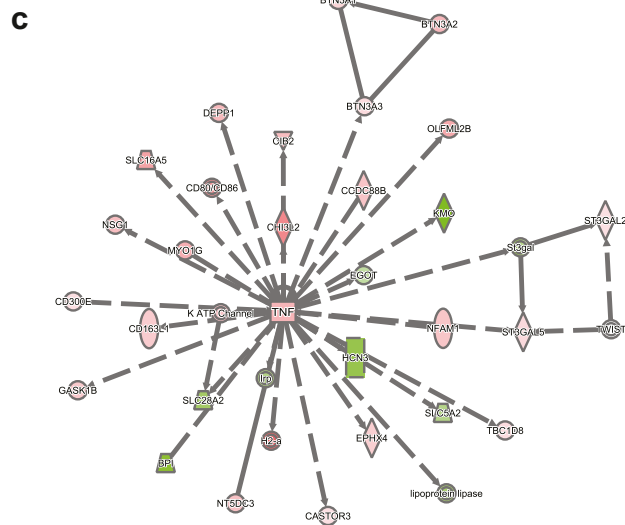
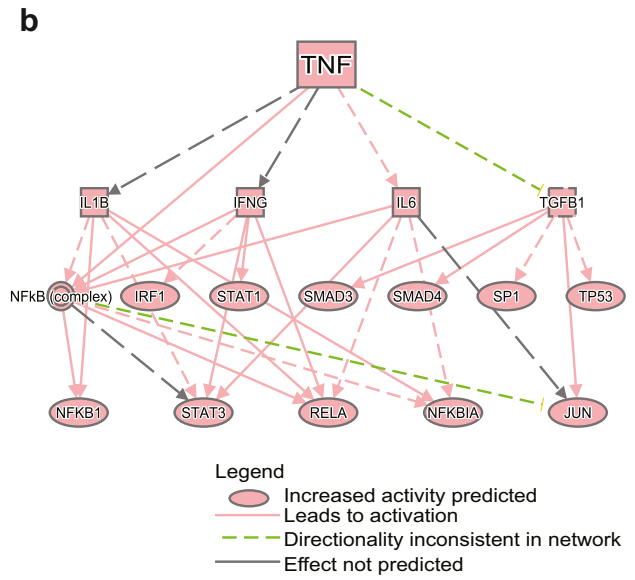
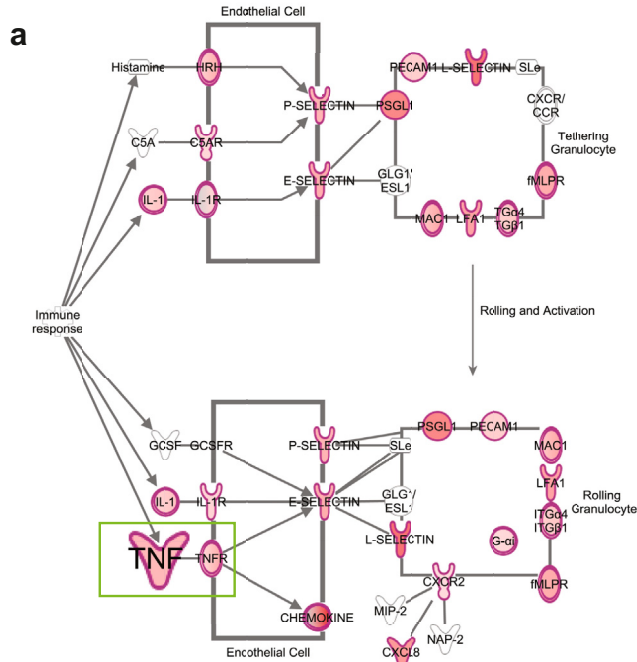
Causal analysis of predicted upstream regulators predicted TNF as the top biological mediator activated in T3 (IPA network Z-score = 13.2, enrichment $P = 2.09E-120$). An expanded causal mechanistic network centered on downstream effects of predicted TNF activation (Figure 3b) explained 48% (1299 of 2721) of the differentially expressed genes between T3 and T1 and 2. Regulated transcripts included multiple transcription factors previously implicated in chronic kidney disease progression, such as nuclear factor kappa B (including NFκB 1 (p105/p50), RELA (p65) subunits)^{11,31,32} and signal transducer and activator of transcription (STAT1 and 3).³³ In the gene interaction network analysis, TNF was identified as the hub gene connecting the T3 regulated gene set (Figure 3c). Mapping the upstream regulators using differential expression profiles from each cohort (Supplementary Table S1A) recapitulated the NEPTUNE signal in the ERCB and H3Africa cohorts, with TNF identified as the top upstream regulator (Supplementary Table S1B).

Next, previously published cell-selective transcripts from human kidney single-cell RNA-seq data sets²⁶ were used to interrogate the cluster-specific tubulointerstitial expression profiles in NEPTUNE. The top 10 genes selectively enriched in kidney cell types²⁶ served as cell-type-specific markers. Bulk RNA-seq expression data were filtered for markers from each cell type to see which cell types contributed most to the

transcriptional signal in T3. Increased contributions in T3 were observed from kidney cells (fibroblasts, endothelial, parietal epithelial, ascending thin loop of Henle, and descending loop of Henle) and immune cell lineages, whereas genes specific for proximal tubules, intercalated cells, thick ascending loop of Henle, distal convoluted tubule, connecting tubule, principal and transitioning cells were expressed at lower levels in T3 (Figure 3d). Taken together, these findings demonstrate that TNF activation in T3 represents a molecular signature derived from both resident kidney and immune cells.

Patient-level TNF activation score and relationship to cluster information

Multiple lines of evidence converged on TNF; therefore, individual-level kidney TNF activation was assessed. Using a rich knowledge base,³⁴⁻³⁶ *in silico* analysis extracted a set of 272 genes causally downstream of TNF activation (Supplementary Table S2). Expression of these 272 genes was used as the readout of TNF activation in kidney biopsies. A TNF activation score was calculated for each participant^{19,33,37,38} and evaluated across the 3 cohorts (Figure 4a). Consistent with TNF activation accounting for the clustering, the range of TNF activation scores were similar, with the highest scores in cluster T3 (Figure 4a). The TNF activation score was also calculated from glomerular samples and found to be strongly correlated with



ATL	ascending thin loop of Henle
CNT	Connecting tubule
DCT	Distal convoluted tubule
DN	Distal nephron
DTL	Descending loop of Henle
DS	Disease specific
DS_TAL	Disease specific thick ascending loop of Henle
EC	Endothelial cell
IC	Intercalated cell
MC	Mesangial cell
PC	Principal cell
PEC	Parietal epithelial cell
POD	Podocyte
PT	Proximal tubular epithelial cell
TAL	Thick ascending loop of Henle
vSMC	Vascular smooth muscle cells
tPC_IC	Transitional principal intercalated cell

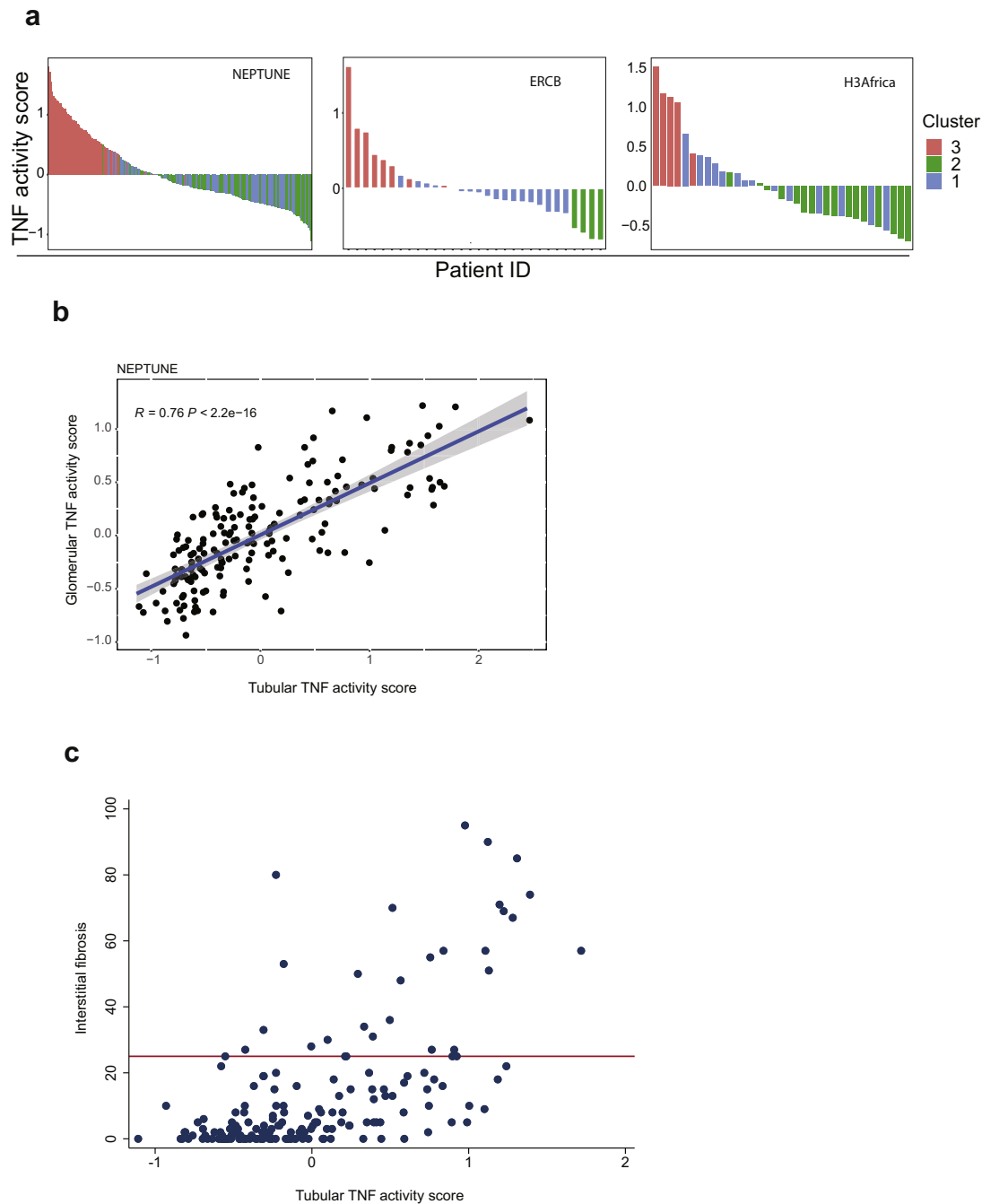


Figure 4 | Tumor necrosis factor (TNF) activity scores across all profiled participants. (a) From the indicated cohorts colored by cluster membership in tubular transcriptomes. (b) Pearson's correlation of TNF activity scores from the glomeruli (y-axis) and tubular (x-axis) transcriptomes in the same North American Nephrotic Syndrome Study Network (NEPTUNE) participants. (c) Correlation of the TNF activity score from the tubular transcriptome with interstitial fibrosis. The horizontal bar (red) indicates 25% interstitial fibrosis. ERCB, European Renal cDNA Bank; H3Africa, Human Heredity and Health in Africa Kidney Disease Research Network cohort.

Figure 3 | Molecular and functional context of cluster T3 expression profiles. Differential expression profiles from T3 compared with T1 and T2 in the North American Nephrotic Syndrome Study Network (NEPTUNE) cohort were generated, and enrichment analysis was performed using Ingenuity Pathways Analysis. (a) Granulocyte adhesion and diapedesis was the top enriched canonical pathway; a subset of the pathway is shown highlighting tumor necrosis factor (TNF) as an input to the pathway. Genes highlighted in red were upregulated in the differential expression profile. (b) A mechanistic network of predicted upstream regulators from the differential expression profile indicating TNF as an input. (c) TNF was identified in a gene interaction network (red indicates that the gene was upregulated in the differential expression profile, whereas green indicates downregulation). (d) Cell selective gene expression markers were previously identified²⁶ and were intersected with voom-transformed gene (row) normalized expression data (yellow indicates higher expression, blue indicates lower expression) to elucidate probable cell contribution to differential expression profiles.

Table 2 | Unadjusted and adjusted Cox proportional hazards models for composite of end-stage kidney disease and 40% decline in eGFR from baseline in the NEPTUNE study

Models	Predictor	Unadjusted model		Adjusted for MCD/FSGS		Adjusted for MCD/FSGS, eGFR, and UPCR	
		HR (95% CI)	P value	HR (95% CI)	P value	HR (95% CI)	P value
Model 1: cluster membership	Cluster 1	Ref.		Ref.		Ref.	
	Cluster 2	1.7 (0.6, 5.1)	0.34	1.6 (0.5, 4.8)	0.40	2.3 (0.69, 7.57)	0.18
	Cluster 3	5.2 (1.9, 14.5)	0.001	4.5 (1.6, 12.9)	0.005	3.80 (1.1, 13.1)	0.035
Model 2: TNF activation score ^a	TNF activation score	2.6 (1.5, 4.4)	0.001	2.3 (1.3, 4.1)	0.003	1.7 (0.9, 3.5)	0.12

CI, confidence interval; eGFR, estimated glomerular filtration rate (ml/min per 1.73 m²); FSGS, focal segmental glomerulosclerosis; HR, hazard ratio; MCD, minimal change disease; NEPTUNE, North American Nephrotic Syndrome Study Network; TNF, tumor necrosis factor; UPCR, urine protein-to-creatinine ratio (mg/mg).

^aHR for increase in Z-score by 1.

the tubulointerstitial TNF activation score in the 2 cohorts where matched gene expression samples were available (Figure 4b). A TNF Z-score was generated using the PROGENy TNF-pathway signature gene set.³⁹ This 98-gene signature shared 41 genes with our *in silico* TNF signature. Both signatures were strongly correlated with one another ($R^2 > 0.94$, $P < 0.0001$) in the tubulointerstitial NEPTUNE transcriptomic data.

Association of cluster 3 and TNF activation with IF and clinical outcomes

The Spearman correlation of TNF activation scores with the severity of IF in NEPTUNE was significant ($n = 179$, $\rho = 0.59$, $P < 0.001$; Figure 4c). However, among the 148 participants with minimal IF (<25% of the kidney cortex), elevated TNF activation scores (TNF activation score >0) were observed in 47 (32%), indicating that the TNF activation score may be more sensitive to the early signs of kidney damage that are not yet visible by histopathologic examination.

To evaluate the extent to which the molecular information from the kidney tissue captured the variability in loss of eGFR over time observed in T3 versus T1 and 2, a survival model was fit separately with cluster membership (model 1, Table 2) and TNF activation score (model 2, Table 2) as primary predictors of interest in NEPTUNE. After adjustments for diagnosis (MCD vs. FSGS), baseline eGFR and UPCR, cluster 3 was associated with a higher hazard of reaching the composite outcome (HR: 3.8, $P = 0.035$). T2 was not significantly different from T1. Similarly, an increase in TNF activation score was associated with higher hazard of the composite outcome (unadjusted HR: 2.6, $P < 0.001$). After adjusting for diagnosis, the HR remained elevated (2.3, $P = 0.003$). The association was attenuated after further adjustment for eGFR and UPCR (HR: 1.7, $P = 0.12$), suggesting that these factors may be on the causal pathway of GFR decline.

Identification of noninvasive surrogates of TNF activation

Based on prior work,⁴⁰ an intrarenal pathway activation signal might be reflected in participants' urine profiles. In NEPTUNE, genes in the TNF activation signature were cross-referenced with the urine proteomic profile. Fourteen genes in the TNF activation network had corresponding

urinary proteins (Figure 5a). Of these, intrarenal gene expression of *CCL2* and *TIMP1* correlated with urine protein levels ($r = 0.58$, $P < 0.0001$ and $r = 0.50$, $P < 0.0001$, respectively). Urinary MCP-1 (the protein encoded by *CCL2*) and TIMP-1 were also correlated with the TNF activation score ($P < 0.0001$, $r \geq 0.50$ for both biomarkers; Figure 5b and c, respectively). Mean levels of both markers were higher in MCD and FSGS participants in cluster T3 (Supplementary Figure S4). Thus, these 2 urine proteins were identified as potential noninvasive surrogates reflective of intrarenal TNF activation.

TNF effect on kidney organoids

Human organoids were used to further support the relationship of the noninvasive surrogate markers to intrarenal TNF activation. TNF treatment of organoids resulted in an early, dose-dependent increase in TNF activation scores (3 hours), which was slightly dampened but sustained for 20 hours in culture (Figure 6a). TNF activation was reflected in the upregulation of *CCL2* and *TIMP1* mRNA expression (Figure 6b) followed by increased detection of the encoded proteins MCP-1 and TIMP-1 in the organoid culture medium (Figure 6c).

TNF activation and expression of surrogate markers in kidney cells

To test the cellular source of the noninvasive surrogate markers in human kidney biopsies, single-nucleus RNA-seq analysis of 10 NEPTUNE biopsies, 5 with high and 5 with moderate-to-low TNF activation scores in the tubulointerstitial profiles, was performed (Supplementary Table S3). The analysis identified 22 unique nuclear clusters representing the major cell types of the kidney (Figure 7a²⁸). In the TNF High samples, cell-type-specific gene expression for both *CCL2* and *TIMP1* were higher across both immune and intrinsic kidney cell types (Figure 7B), consistent with findings from kidney organoids. Thus, the TNF-responsive surrogate markers reflect alterations in inflammatory and resident kidney cells in participants with TNF pathway activation.

Predictive ability of surrogate markers

NEPTUNE participants with TNF activation scores, and urinary cytokine measurements obtained within 45 days after

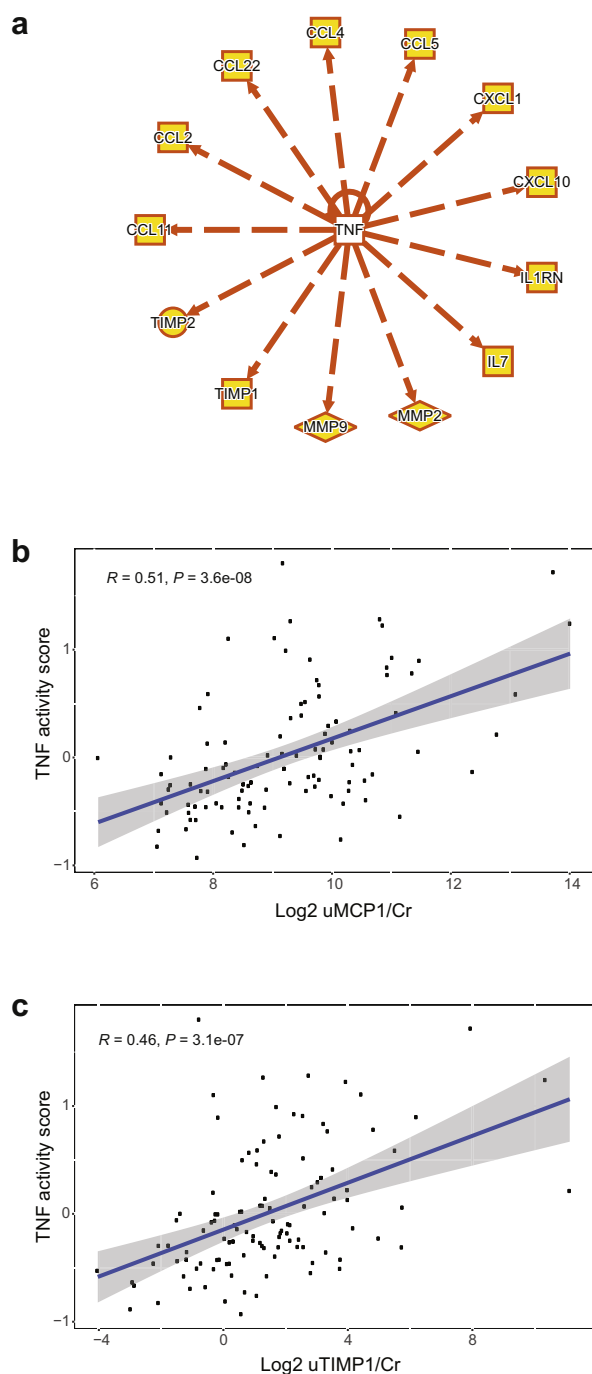


Figure 5 | Noninvasive surrogate selection for tumor necrosis factor (TNF) activation. (a) Fourteen genes upregulated in cluster T3, were downstream of TNF activation, as characterized by curated cause and effect relationships, and were present on the Luminex panel used to profile urine profile from North American Nephrotic Syndrome Study Network (NEPTUNE) participants. The TNF activation score plotted against (b) Log_2 uMCP1/Cr and (c) Log_2 uTIMP1/Cr. MCP-1, monocyte chemoattractant protein-1; TIMP-1, tissue inhibitor of metalloproteinases-1.

biopsy (N = 90), were included in predictive models. Using a combination of urine biomarkers (MCP-1 and TIMP-1), eGFR and UPCR, a predicted TNF score was calculated and

highly correlated with the transcriptionally derived intrarenal TNF activation score ($r = 0.61$, $P < 0.001$; Figure 8). Thus, a noninvasive biomarker signature of MCP-1 and TIMP-1, coupled with routinely obtained clinical information, predicts intrarenal TNF activation profiles in participants with FSGS and MCD.

DISCUSSION

This study used tissue transcriptomics to address the heterogeneity in disease progression under routine clinical care, in children and adults with biopsied MCD and FSGS, to agnostically identify patient subgroups with a shared molecular signature. In the subgroup with the highest risk of eGFR loss, activation in the kidney of a targetable pathway was identified that could be quantified at an individual level, and predicted noninvasively, through urine surrogate markers. Such approaches for identifying molecular markers provide a strategy for precision medicine in nephrology, where patients can be matched to mechanistically relevant therapies.²

For the first time, from a cluster of participants with shared molecular profiles in 3 geographically diverse cohorts, a subgroup of high-risk participants, comprising both MCD and FSGS diagnoses, was identified. Clustering remained consistent when limiting to those with low levels of IF and, after adjusting for diagnosis, eGFR and UPCR, this subgroup had increased risk of GFR loss. This suggests that transcriptomic data capture prognostic information not currently captured by clinical-pathologic evaluation and potential disease pathways not targeted by current treatments. The pathways within the subgroup's molecular profile could represent a variety of biological processes, including both disease initiating and progression mechanisms, both of which could be valuable targets for therapy.

The kidney tissue molecular profile of the poor outcome subgroup centered on TNF activation, a cytokine linked to a range of diseases.^{41–44} From several lines of evidence, including human and animal studies in kidneys,^{45,46} TNF is produced in immune and resident kidney cells,^{47,48} has been implicated early in disease causation^{49,50} and progression,^{44,47,49,51} but has not been implemented in clinical care. Although TNF activation was associated with the degree of fibrosis in this study, many participants without significant scarring had elevated TNF activation scores, demonstrating that pathway activation may occur early in the disease course. Two candidate urine markers of TNF activation were identified: MCP-1, a marker of active inflammation,⁵² and TIMP-1, associated with tissue remodeling and scarring.⁵³ These markers were elevated in the poor outcome cluster and, along with existing clinical measures, accurately predicted intrarenal TNF activation. Cell-specific transcriptional signals characterizing the poor outcome cluster were derived from both infiltrating immune cells and resident kidney cells, including endothelial cells. This was confirmed in the single-nucleus RNA-seq data where participants with high TNF scores showed increased expression of *CCL2* and *TIMP1* across multiple cell types. In addition, TNF-treated

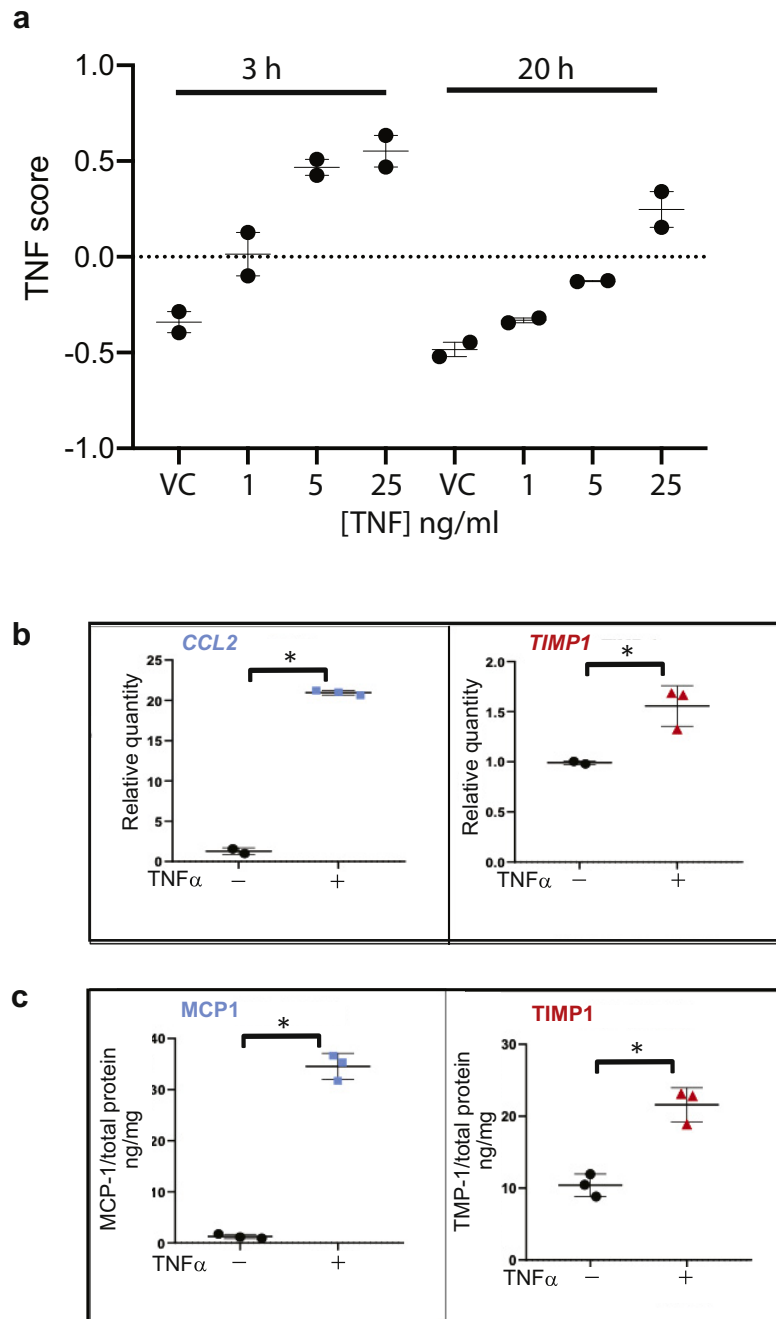


Figure 6 | Tumor necrosis factor (TNF) effects on kidney organoids and surrogate markers. TNF directly stimulates TNF activation and expression of the selected surrogate markers in human pluripotent stem-cell-derived kidney organoids. (a) TNF activation scores were calculated from bulk RNA-sequencing data obtained from kidney organoids treated with vehicle control (VC) or 1, 5, 25 ng/ml TNF for 3 or 20 hours. Quantification of (b) *CCL2* (left) and *TIMP1* (right) transcript levels in kidney organoid cell lysates by quantitative real-time polymerase chain reaction relative to control, and of (c) Monocyte chemoattractant protein-1 (MCP-1; left) and tissue inhibitor of metalloproteinases-1 (TIMP-1; right) protein levels in kidney organoid culture supernatant by the enzyme-linked immunosorbent assay normalized to total protein, generated from the same samples after treatment with 5 ng/ml TNF or VC for 24 hours. Each data point was generated from a unique sample and represents the average of analysis in triplicate. Long bar, mean; short bar, 1 SD; **P* value < 0.05 by Student's *t* test. Representative experiment (1 of 4 independent) shown.

organoids had increased TNF pathway activation scores, transcript and protein levels of TIMP-1 and MCP-1.

Case reports and small studies suggest that anti-TNF therapy may be effective in a subset of patients with nephrotic syndrome, but intrarenal TNF activation was not

assessed.^{54–56} The FONT trial (Novel Therapies for Resistant FSGS) tested the TNF inhibitor adalimumab in patients with multidrug-resistant FSGS.^{57,58} Of the 17 patients treated in the combined phase I and phase II studies, 4 patients had a $\geq 50\%$ reduction in proteinuria; 2 patients achieved

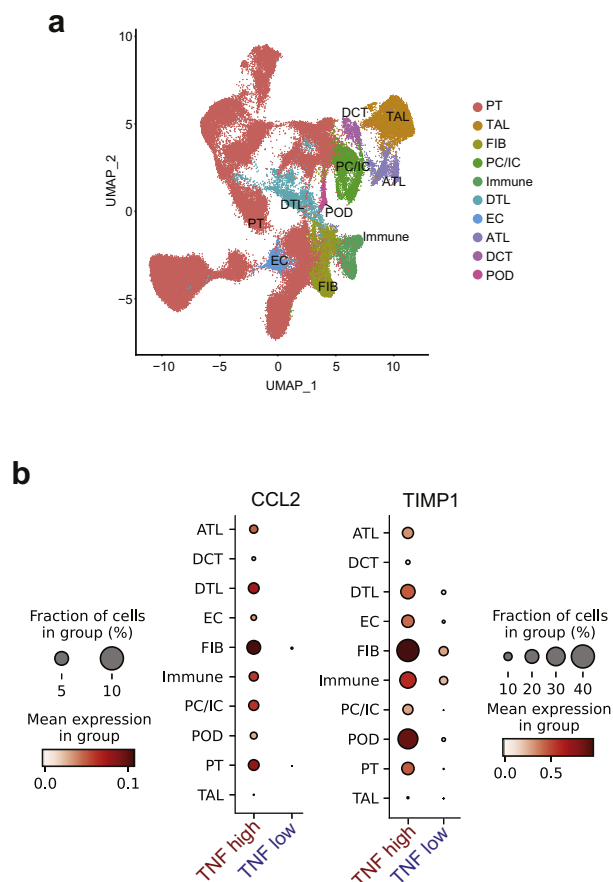


Figure 7 | Tumor necrosis factor (TNF) effects on kidney and immune cell types by single-nucleus RNA sequencing (snRNA-seq) from glomerular-depleted biopsies. (a) Uniform Manifold Approximation and Projection (UMAP) plot of snRNA-seq profiles from TI of selected North American Nephrotic Syndrome Study Network (NEPTUNE) participants found to have elevated TNF activation scores (TNF High) and low-to-moderate TNF activation scores (TNF Low) and (b) single nuclear cluster expression of *CCL2* and *TIMP1* by TNF activation status. Cell-type-specific markers were based on Lake *et al.*²⁸ ATL, ascending thin limb cells; *CCL2*, CC chemokine ligand 2; DCT, distal convoluted tubule cells; DTL, descending thin limb cells; EC-GC, glomerular endothelial cells; FIB, fibroblast cells; Immune, several types of immune cells; PC/IC, principal cells/intercalated cells; POD, podocytes; PT, proximal tubule cells; TAL, thick ascending limb cells; *TIMP-1*, tissue inhibitor of metalloproteinases-1.

dramatic improvements, from UPCR of 17 to 0.6 mg/mg in one and from 3.6 to 0.6 mg/mg in the other. Although the study was considered unsuccessful in demonstrating the efficacy of anti-TNF therapy for patients with FSGS as a group, a response in any patient with this severe phenotype is notable and consistent with underlying biologic heterogeneity within the diagnosis. Other clinical trials in MCD and FSGS have also observed variable responses to other interventions.^{59,60}

These examples highlight the need for precision medicine and for clinical trials to incorporate markers (serum, urine, or genetic), indicating activation of the targeted injury pathway to ensure alignment of the molecular profile of participants

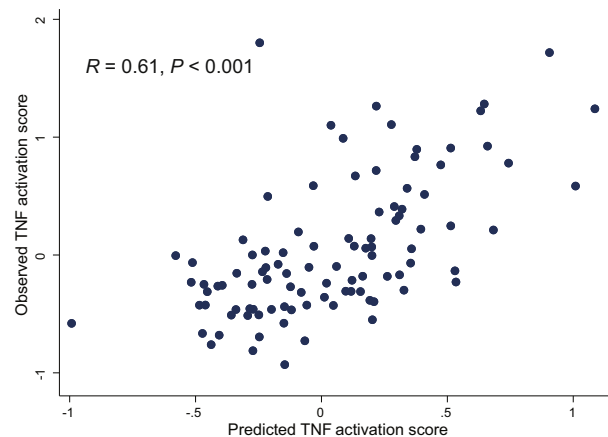


Figure 8 | Correlation of observed tumor necrosis factor (TNF) activation score with a predicted score based on urinary biomarkers and clinical features. Linear regression models were used to generate predicted tissue TNF activation scores based on estimated glomerular filtration rate, urine protein-to-creatinine ratio, urinary tissue inhibitor of metalloproteinases-1, and urinary monocyte chemoattractant protein-1. Correlation was 0.61, P value < 0.001 .

with that of the intervention. Molecular categorization could be combined with consensus clustering based on clinical and laboratory data, as outlined here for nephrotic syndrome, and recently applied to the Chronic Renal Insufficiency Cohort,⁶¹ for precise delineation of patient prognosis and optimization of therapy.

The subgroup of highest clinical need, those with the greatest risk of GFR loss, was the focus for this initial study. Tubulointerstitial damage and fibrosis have been shown to strongly associate with eGFR decline and treatment response across diagnoses.^{19,62–64} Therefore, although MCD and FSGS are glomerular diseases, the premise for this study was that pathways associated with disease progression were more likely to be detected in the tubulointerstitial profiles. Nevertheless, the TNF activation signals in the glomerular and tubular compartments were strongly correlated, capturing similar activation in both compartments. Further, even when only the participants with low fibrosis were clustered, their high-risk subgroup membership persisted. Therefore, the tubulointerstitial TNF pathway merits investigation and may represent both disease initiating and chronic progression mechanisms in glomerular diseases.

Several limitations of the present study are acknowledged. This study included only biopsy-proven MCD and FSGS. The TNF pathway and associated urine markers are likely relevant to other kidney diseases that could be addressed in future studies using this pipeline. Relatedly, this study included all MCD and FSGS participants to be broadly inclusive of the spectrum of presentation at the time of a clinical biopsy. However, patients with MCD, particularly children, who respond well to therapy and may not receive a clinical biopsy are not represented in this cohort. Similar analyses could identify pathways relevant within clinical subgroups of these

diagnoses (e.g., only those with high degrees of proteinuria). Future work using non-tissue-based omic technology could identify molecular subclusters in nonbiopsied patients, not included here. Genetic information is expanding our understanding of nephrotic syndrome. However, in NEPTUNE, a low frequency of mutations in 21 monogenic nephrotic syndrome-associated genes were detected,⁶⁵ and likely prevented us from finding an association of TNF with monogenic glomerular diseases. Similar data are unavailable for ERCB and H3Africa. In many patients, a single pathway is unlikely to drive disease progression and additional or combination therapies may be appropriate. Future work using this pipeline and data from this study can uncover additional pathways and surrogate markers relevant to each of the tubular and glomerular transcriptomic clusters.

As next steps, clinical studies are needed to validate the use of predicted TNF activation scores as a target engagement biomarker during the treatment of FSGS and other glomerular diseases. Reprising the FONT trial design by limiting trial eligibility to patients with high predicted TNF pathway activation would enable the assessment of response to TNF inhibition, stratified by TNF activation levels. A phase IIa proof of concept trial with this design has been initiated for children and adults with biopsy-proven FSGS and MCD (clinicaltrials.gov/NCT04009668).

In conclusion, this study provides a road map for implementing precision medicine in primary podocytopathies. It identified a molecularly defined subset of patients with nephrotic syndrome who have poor clinical outcomes and increased activation of a targetable pathway, TNF, as a key driver of disease progression. Noninvasive markers, validated in an organoid model system, are available to identify the participants with TNF activation, an approach currently being tested in an interventional trial. The concepts developed here for FSGS/MCD, and the TNF pathway represents a first step toward a comprehensive map of targetable pathways for glomerular diseases and a move toward precision medicine where the right medicine is administered to the right patient with glomerular disease.

DISCLOSURE

MK reports grants from the National Institutes of Health (NIH), Chan Zuckerberg Initiative, JDRF, AstraZeneca, NovoNordisk, Eli Lilly, Gilead, Goldfinch Bio, Janssen, Boehringer Ingelheim, Moderna, European Union Innovative Medicine Initiative, Cert, Chinook, amfAR, Angion, RenalytixAI, Travere, Regeneron, and IONIS, outside the submitted work. In addition, he has a patent PCT/EP2014/073413 "Biomarkers and methods for progression prediction for chronic kidney disease" licensed. Also, outside of submitted work, LHM has served on the advisory board of Reata Pharmaceuticals, Calliditas Therapeutics, Chinook Therapeutics, and Travere Therapeutics. SE reports grant support from AstraZeneca, NovoNordisk, Eli Lilly, Gilead, Janssen, Moderna, Cert, Chinook, amfAR, Angion, and IONIS, outside the submitted work. HT consults for Travere Therapeutics, Goldfinch Bio, Akebia, Natera, Otsuka, and Chemocentryx. KLG serves on Reata CKD Advisory Board and the Travere Inc. FSGS and IgA Advisory WorkGroup. VKD reports funding from Novartis, honoraria from UpToDate, and has served on the advisory board of Retrophin and

Bayer. JCL reports grants from Dicerna, Allena, Orfan-Bridgebio, Synlogic, Novobiome, OxThera, Oxidien, Alnylam, and Federation Bio, outside the submitted work. LAG reports grants from Reata Pharmaceuticals and Vertex Pharmaceuticals. He has served as a paid consultant for Roche Pharmaceuticals. He is a paid member of a data safety monitoring board for Travere Pharmaceuticals. DSG reports grants from Travere Therapeutics, Reata, Goldfinch Bio, Novartis, and Boehringer Ingelheim and serves on advisory or consultancy through the University of Michigan with Roche, Genentech, AstraZeneca, and Vertex. All the other authors declared no competing interests.

ACKNOWLEDGMENTS

We thank Dr. Lalita Subramanian for help with writing, editing, and formatting this manuscript. The Nephrotic Syndrome Study Network Consortium (NEPTUNE), U54-DK-083912, is a part of the National Institutes of Health (NIH) Rare Disease Clinical Research Network (RDCRN), supported through collaboration between the Office of Rare Diseases Research, National Center for Advancing Translational Sciences, and the National Institute of Diabetes, Digestive, and Kidney Diseases (NIDDK). Additional funding and/or programmatic support for this project has also been provided by the Else Kröner-Fresenius Foundation (ERCB), University of Michigan, the NephCure Kidney International and the Halpin Foundation, and the Applied Systems Biology Core at the University of Michigan George M. O'Brien Kidney Translational Core Center (2P30-DK-08194). LHM is supported through funding from NIH/NIDDK, K08 DK115891-01. We acknowledge the role of the H3Africa Consortium in making this research possible through the sharing of data and knowledge. The NIH (USA) and Wellcome Trust (UK) have provided the core funding for the H3Africa Consortium, and more information is available at <https://h3africa.org/>. This research was supported by the following grants from NIH/National Human Genome Research Institute (NHGRI)/NIDDK: H3Africa Kidney Disease Study (U54 HG006939), H3Africa Kidney Disease Cohort Study (U01 DK107131), H3Africa Kidney Disease Collaborative Centers (9U54 DK116913). The views expressed in this paper do not represent the views of the H3Africa Consortium or their funders. ERCB, NEPTUNE, and H3Africa contributing members are listed in the Supplementary Acknowledgment.

AUTHOR CONTRIBUTIONS

All co-authors have contributed to the manuscript. LHM, SE, MK, KRT, PHN, JCL, DCC, DA, KLG, JRS, HNR, SMB, LB, RAL, JBH, DSG, JLH, LBH, HT, CAG conceptualized this study; LHM, SE, VB, WJ, SMB, JLH, J-JL, FMA, MMO, VN, PJM contributed to data curation; LHM, SE, FMA, PJM, WJ, JLH did the formal analysis; LHM, SE, MK, VB, DA, JCL, JRS, AF, LBH, RAL, LB, DSG, AOO were involved in funding acquisition; LHM, SE, MK, PJM, KRT, VB, KVL, LB, SGA, ADA, TS, C-SW, FCF, CLT, DCC, WJ, DA, KLG, BG, KEM, LBH, SMB, RAL, JBH, MAA, J-JL investigated the findings; FMA, SM, PJM, BG, JBH, VN, SE, JLH developed the methodology; LHM, SE, KRT, VB, FE, KKS, TS, FCF, SMV, DA, KLG, KEM were involved in project administration; KVL, LAG, SGA, ADA, AA, LHM, JCL, FCF, SMV, CLT, DA, KLG, BG, AF, KEM, HNR, LBH, RAL, JBH, MAA, J-JL, MK provided resources; SE, FMA, PJM worked on software used in the study; SE, FE, FMA, PJM performed bioinformatic processing and analyses in the study; LHM, SE, KRT, VB, ADA, AA, JCL, VKD, KLG, AF, KEM, HNR, LBH, RAL, MK, JLH supervised the study; VB, ADA and WJ worked on study validation; NLW, VV-W, ECT, JES performed kidney organoid experiments; BG, RM, PJM, EAO coordinated processing and analysis of single nuclear RNA-seq samples; LHM, SE, VB, CBS, FMA, ADA, PJM, KEM, and LBH helped with visualization; LHM, SE, VB, PJM, and JLH wrote the original draft; all authors reviewed and provided valuable feedback on the manuscript.

SUPPLEMENTARY MATERIAL

Supplementary File (PDF)

Supplementary Acknowledgments. European Renal cDNA Bank (ERCB) members at the time of the study, Members of the Nephrotic Syndrome Study Network (NEPTUNE) at the time of the study, and Members of the Human Heredity and Health in Africa Kidney Disease Research Network cohort (H3 Africa).

Supplementary Methods.

Supplementary References.

Figure S1. Cluster dendrogram and assignment of minimal change disease (MCD) and focal segmental glomerulosclerosis (FSGS) participants based on kidney biopsy tubulointerstitial gene expression data in North American Nephrotic Syndrome Study Network (NEPTUNE), European Renal cDNA Bank (ERCB), and Human Heredity and Health in Africa Kidney Disease Research Network cohort (H3 Africa).

Figure S2. Comparison of cluster assignment and clinical measures in North American Nephrotic Syndrome Study Network (NEPTUNE) and European Renal cDNA Bank (ERCB) using glomerular compartment expression data.

Figure S3. Comparison of clinical factors and cluster assignment across cohorts.

Figure S4. Urine marker levels by diagnosis and cluster.

Table S1A. List of differentially expressed genes (absolute FC >1.5, $q < 0.05$) in cluster 3 versus clusters 1 and 2, in each cohort, used for enrichment analyses.

Table S1B. Predicted upstream regulators based on DEG profiles of patients in cluster 3 relative to clusters 1 and 2.

Table S2. Genes and gene products activated by tumor necrosis factor (TNF) used to generate the TNF activation score.

Table S3. Clinical characteristics of North American Nephrotic Syndrome Study Network (NEPTUNE) participants with biopsies used for single-nucleus RNA-seq.

REFERENCES

- Kidney Disease: Improving Global Outcomes (KDIGO) Glomerular Diseases Work Group. KDIGO 2021 clinical practice guideline for the management of glomerular diseases. *Kidney Int.* 2021;100(4S):S1–S276.
- D'Agati VD, Alster JM, Jennette JC, et al. Association of histologic variants in FSGS clinical trial with presenting features and outcomes. *Clin J Am Soc Nephrol.* 2013;8:399–406.
- Rosenberg AZ, Kopp JB. Focal segmental glomerulosclerosis. *Clin J Am Soc Nephrol.* 2017;12:502–517.
- Gipson DS, Troost JP, Lafayette RA, et al. Complete remission in the nephrotic syndrome study network. *Clin J Am Soc Nephrol.* 2016;11:81–89.
- Trachtman H, Nelson P, Adler S, et al. DUET: a phase 2 study evaluating the efficacy and safety of sparsentan in patients with FSGS. *J Am Soc Nephrol.* 2018;29:2745–2754.
- Janiaud P, Serghiou S, Ioannidis JPA. New clinical trial designs in the era of precision medicine: an overview of definitions, strengths, weaknesses, and current use in oncology. *Cancer Treat Rev.* 2019;73:20–30.
- Collins FS. Reengineering translational science: the time is right. *Sci Transl Med.* 2011;3:90cm17.
- Eddy S, Mariani LH, Kretzler M. Integrated multi-omics approaches to improve classification of chronic kidney disease. *Nat Rev Nephrol.* 2020;16:657–668.
- Barisoni L, Nast CC, Jennette JC, et al. Digital pathology evaluation in the multicenter Nephrotic Syndrome Study Network (NEPTUNE). *Clin J Am Soc Nephrol.* 2013;8:1449–1459.
- Yasuda Y, Cohen CD, Henger A, et al. Gene expression profiling analysis in nephrology: towards molecular definition of renal disease. *Clin Exp Nephrol.* 2006;10:91–98.
- Schmid H, Boucherot A, Yasuda Y, et al. Modular activation of nuclear factor-kappaB transcriptional programs in human diabetic nephropathy. *Diabetes.* 2006;55:2993–3003.
- Osafo C, Raji YR, Burke D, et al. Human Heredity and Health (H3) in Africa Kidney Disease Research Network: a focus on methods in Sub-Saharan Africa. *Clin J Am Soc Nephrol.* 2015;10:2279–2287.
- Osafo C, Raji YR, Olanrewaju T, et al. Genomic approaches to the burden of kidney disease in Sub-Saharan Africa: the Human Heredity and Health in Africa (H3Africa) Kidney Disease Research Network. *Kidney Int.* 2016;90:2–5.
- Gadegbeku CA, Gipson DS, Holzman LB, et al. Design of the Nephrotic Syndrome Study Network (NEPTUNE) to evaluate primary glomerular nephropathy by a multidisciplinary approach. *Kidney Int.* 2013;83:749–756.
- Levey AS, Bosch JP, Lewis JB, et al. A more accurate method to estimate glomerular filtration rate from serum creatinine: a new prediction equation. Modification of Diet in Renal Disease Study Group. *Ann Intern Med.* 1999;130:461–470.
- Schwartz GJ, Work DF. Measurement and estimation of GFR in children and adolescents. *Clin J Am Soc Nephrol.* 2009;4:1832–1843.
- Ng DK, Schwartz GJ, Schneider MF, et al. Combination of pediatric and adult formulas yield valid glomerular filtration rate estimates in young adults with a history of pediatric chronic kidney disease. *Kidney Int.* 2018;94:170–177.
- Zee J, Mansfield S, Mariani LH, Gillespie BW. Using all longitudinal data to define time to specified percentages of estimated GFR decline: a simulation study. *Am J Kidney Dis.* 2019;73:82–89.
- Grayson PC, Eddy S, Taroni JN, et al. Metabolic pathways and immunometabolism in rare kidney diseases. *Ann Rheum Dis.* 2018;77:1226–1233.
- Barisoni L, Troost JP, Nast C, et al. Reproducibility of the NEPTUNE descriptor-based scoring system on whole-slide images and histologic and ultrastructural digital images. *Mod Pathol.* 2016;29:671–684.
- Edgar R, Domrachev M, Lash AE. Gene Expression Omnibus: NCBI gene expression and hybridization array data repository. *Nucleic Acids Res.* 2002;30:207–210.
- Wilkerson MD, Hayes DN. ConsensusClusterPlus: a class discovery tool with confidence assessments and item tracking. *Bioinformatics.* 2010;26:1572–1573.
- Monti S, Tamayo P, Mesirov JP, Golub T. Consensus clustering: a resampling-based method for class discovery and visualization of gene expression microarray data. *Mach Learn.* 2004;52:91–118.
- Ritchie ME, Phipson B, Wu D, et al. limma powers differential expression analyses for RNA-seq and microarray studies. *Nucleic Acids Res.* 2015;43:e47.
- Calvano SE, Xiao W, Richards DR, et al. A network-based analysis of systemic inflammation in humans. *Nature.* 2005;437:1032–1037.
- Menon R, Otto EA, Hoover P, et al. Single cell transcriptomics identifies focal segmental glomerulosclerosis remission endothelial biomarker. *JCI Insight.* 2020;5:e133267.
- Lake BB, Chen S, Hoshi M, et al. A single-nucleus RNA-seq pipeline to decipher the molecular anatomy and pathophysiology of human kidneys. *Nat Commun.* 2019;10:2832.
- Lake BB, Menon R, Winfree S, et al. An atlas of healthy and injured cell states and niches in the human kidney. *bioRxiv.* 2021, 2021.2007.2028.454201.
- Harder JL, Menon R, Otto EA, et al. Organoid single cell profiling identifies a transcriptional signature of glomerular disease. *JCI Insight.* 2019;4:e122697.
- Krämer A, Green J, Pollard J Jr, Tugendreich S. Causal analysis approaches in Ingenuity Pathway Analysis. *Bioinformatics.* 2014;30:523–530.
- Wiggins JE, Patel SR, Shedden KA, et al. NFkappaB promotes inflammation, coagulation, and fibrosis in the aging glomerulus. *J Am Soc Nephrol.* 2010;21:587–597.
- Martini S, Nair V, Keller BJ, et al. Integrative biology identifies shared transcriptional networks in CKD. *J Am Soc Nephrol.* 2014;25:2559–2572.
- Tao J, Mariani L, Eddy S, et al. JAK-STAT signaling is activated in the kidney and peripheral blood cells of patients with focal segmental glomerulosclerosis. *Kidney Int.* 2018;94:795–808.
- Gupta A, Puri S, Puri V. Bioinformatics unmasks the maneuverers of pain pathways in acute kidney injury. *Sci Rep.* 2019;9:11872.
- Schüler-Toprak S, Häring J, Inwald EC, et al. Agonists and knockdown of estrogen receptor β differentially affect invasion of triple-negative breast cancer cells in vitro. *BMC Cancer.* 2016;16:951.
- Supper J, Gugenmus C, Wollnik J, et al. Detecting and visualizing gene fusions. *Methods.* 2013;59:S24–S28.
- Lee E, Chuang HY, Kim JW, et al. Inferring pathway activity toward precise disease classification. *PLoS Comput Biol.* 2008;4:e1000217.
- Tao J, Mariani L, Eddy S, et al. JAK-STAT activity in peripheral blood cells and kidney tissue in IgA nephropathy. *Clin J Am Soc Nephrol.* 2020;15:973–982.

39. Schubert M, Klinger B, Klünemann M, et al. Perturbation-response genes reveal signaling footprints in cancer gene expression. *Nat Commun.* 2018;9:20.
40. Ju W, Nair V, Smith S, et al. Tissue transcriptome-driven identification of epidermal growth factor as a chronic kidney disease biomarker. *Sci Transl Med.* 2015;7:316ra193.
41. Ware CF. The TNF superfamily-2008. *Cytokine Growth Factor Rev.* 2008;19:183–186.
42. Jäättelä M. Biologic activities and mechanisms of action of tumor necrosis factor- α /cachectin. *Lab Invest.* 1991;64:724–742.
43. Hernandez T, Mayadas TN. Immunoregulatory role of TNF α in inflammatory kidney diseases. *Kidney Int.* 2009;76:262–276.
44. Bakr A, Shokeir M, El-Chenawi F, et al. Tumor necrosis factor- α production from mononuclear cells in nephrotic syndrome. *Pediatr Nephrol.* 2003;18:516–520.
45. McCarthy ET, Sharma R, Sharma M, et al. TNF- α increases albumin permeability of isolated rat glomeruli through the generation of superoxide. *J Am Soc Nephrol.* 1998;9:433–438.
46. Le Berre L, Herve C, Buzelin F, et al. Renal macrophage activation and Th2 polarization precedes the development of nephrotic syndrome in Buffalo/Mna rats. *Kidney Int.* 2005;68:2079–2090.
47. Pedigo CE, Ducasa GM, Leclercq F, et al. Local TNF causes NFATc1-dependent cholesterol-mediated podocyte injury. *J Clin Invest.* 2016;126:3336–3350.
48. Baud L, Fouqueray B, Philippe C, Amrani A. Tumor necrosis factor α and mesangial cells. *Kidney Int.* 1992;41:600–603.
49. Otalora L, Chavez E, Watford D, et al. Identification of glomerular and podocyte-specific genes and pathways activated by sera of patients with focal segmental glomerulosclerosis. *PLoS One.* 2019;14:e0222948.
50. Lee HH, Cho YI, Kim SY, et al. TNF- α -induced inflammation stimulates apolipoprotein-A4 via activation of TNFR2 and NF- κ B signaling in kidney tubular cells. *Sci Rep.* 2017;7:8856.
51. Wen Y, Lu X, Ren J, et al. KLF4 in macrophages attenuates TNF α -mediated kidney injury and fibrosis. *J Am Soc Nephrol.* 2019;30:1925–1938.
52. Kim MJ, Tam FWK. Urinary monocyte chemoattractant protein-1 in renal disease. *Clin Chim Acta.* 2011;412:2022–2030.
53. Ahmed AK, Haylor JL, El Nahas AM, Johnson TS. Localization of matrix metalloproteinases and their inhibitors in experimental progressive kidney scarring. *Kidney Int.* 2007;71:755–763.
54. Peyser A, Machardy N, Tarapore F, et al. Follow-up of phase I trial of adalimumab and rosiglitazone in FSGS: III. Report of the FONT study group. *BMC Nephrol.* 2010;11:2.
55. Raveh D, Shemesh O, Ashkenazi YJ, et al. Tumor necrosis factor- α blocking agent as a treatment for nephrotic syndrome. *Pediatr Nephrol.* 2004;19:1281–1284.
56. Ito S, Tsutsumi A, Harada T, et al. Long-term remission of nephrotic syndrome with etanercept for concomitant juvenile idiopathic arthritis. *Pediatr Nephrol.* 2010;25:2175–2177.
57. Joy MS, Gipson DS, Powell L, et al. Phase 1 trial of adalimumab in Focal Segmental Glomerulosclerosis (FSGS): II. Report of the FONT (Novel Therapies for Resistant FSGS) study group. *Am J Kidney Dis.* 2010;55:50–60.
58. Trachtman H, Vento S, Herreshoff E, et al. Efficacy of galactose and adalimumab in patients with resistant focal segmental glomerulosclerosis: report of the font clinical trial group. *BMC Nephrol.* 2015;16:111.
59. Hogan J, Bomback AS, Mehta K, et al. Treatment of idiopathic FSGS with adrenocorticotrophic hormone gel. *Clin J Am Soc Nephrol.* 2013;8:2072–2081.
60. Yu C-C, Fornoni A, Weins A, et al. Abatacept in B7-1-positive proteinuric kidney disease. *N Engl J Med.* 2013;369:2416–2423.
61. Zheng Z, Waikar SS, Schmidt IM, et al. Subtyping CKD patients by consensus clustering: the Chronic Renal Insufficiency Cohort (CRIC) Study. *J Am Soc Nephrol.* 2021;32:639–653.
62. Zee J, Liu Q, Smith AR, et al. Kidney biopsy features most predictive of clinical outcomes in the spectrum of minimal change disease and focal segmental glomerulosclerosis. *J Am Soc Nephrol.* 2022;33:1411–1426.
63. Kolachalama VB, Singh P, Lin CQ, et al. Association of pathological fibrosis with renal survival using deep neural networks. *Kidney Int Rep.* 2018;3:464–475.
64. Srivastava A, Palsson R, Kaze AD, et al. The prognostic value of histopathologic lesions in native kidney biopsy specimens: results from the Boston Kidney Biopsy Cohort Study. *J Am Soc Nephrol.* 2018;29:2213–2224.
65. Sampson MG, Gillies CE, Robertson CC, et al. Using population genetics to interrogate the monogenic nephrotic syndrome diagnosis in a case cohort. *J Am Soc Nephrol.* 2016;27:1970–1983.